

A Case Study of the Munich Address

Tracing Shifts in Collective Attention Across Europe

Ulf Holmberg

2025-11-18

Abstract

This paper presents an exploratory case study of the Global Consciousness Project 2 (GCP-2) network during U.S. Vice President J. D. Vance's keynote address at the 2025 Munich Security Conference. Using second-by-second data from RNG streams in the UK, Madrid, and from the global network, Vector Error Correction Models were estimated across four separate phases: the live speech (13:30–14:00 UTC), the initial media rollout (14:00–16:00 UTC), the evening uptake (16:00–21:00 UTC) and the Post-Event Drift Phase (21:00–24:00). Across these windows, the results reveal a rotating pattern of adjustment: a strong UK-centered response during the live broadcast, bilateral UK–Madrid coherence as coverage expanded, and a Madrid-anchored equilibrium as continental discussion intensified. These econometric effects were independently corroborated by cumulative-sum deviation plots, which displayed corresponding phase-specific drifts and envelope crossings in each time window. Impulse-response functions further support this sequence, showing a brief local UK → global impulse, followed by distributed reinforcement, and a slower continental stabilization. Taken together, the findings indicate that RNG nodes behave as local transducers of collective attention, registering regionally concentrated cognitive–emotional engagement that subsequently synchronizes across the global network.

Keywords: Global Consciousness Project, Collective Attention, Vector Error Correction Model (VECM), Cumulative Sum (CUSUM) Analysis, Diffusion Dynamics

1. Introduction

At 13:30 UTC on 14 February 2025, U.S. Vice President J. D. Vance addressed European leaders at the Munich Security Conference, declaring that “the era of automatic American protection is over”.¹ Within minutes, the remark dominated English-language media feeds, and within hours it was reframed across Europe as a call for renewed strategic autonomy, an especially charged message given the ongoing conflict on the continent’s eastern border. This rapid cascade of attention, moving from tightly focused real-time viewing to continent-wide interpretive engagement, creates an unusually clear natural experiment for testing whether synchrony of human attention can alter entropy in ways that leave measurable traces in the Global Consciousness Project (GCP) data.

The original Global Consciousness Project (GCP1), launched in 1998, operated a worldwide network of electronic and quantum-based random number generators (RNGs) producing continuous data streams. Over the subsequent two decades, analyses repeatedly found that periods of widespread collective attention, e.g., major terrorist attacks, New Year’s celebrations, mass meditations, and globally broadcast events, tended to coincide with small but statistically detectable departures from chance expectation in the aggregated network. The pattern that motivated the creation of the GCP had emerged in earlier FieldREG experiments and as Nelson et al. (1998) put it, after analyzing portable RNG data collected at group events:

“The results strongly confirm the general hypothesis that environments fostering relatively intense or profound subjective resonance will show larger deviations from expectation.”

Subsequent summaries of the Global Consciousness Project emphasized that the effect is subtle but persistent. Nelson (2001, 2002), for example, reported “small but persistent correlations” between REG/RNG deviations and periods of heightened collective attention, even when events differed widely in emotional tone. Radin (2006) likewise concluded, drawing on both FieldREG and laboratory experiments, that groups “sharing strong emotions or common focus can produce an orderly departure from randomness in nearby REG devices”. Early FieldREG studies (Radin & Nelson, 1989; Nelson et al., 1996) further suggested that attention synchrony in groups as small as a few dozen participants can be associated with measurable ordering in RNG outputs placed in the same room.

Although the dominant interpretation in the GCP community has been that these effects are *nonlocal*—that is, largely independent of physical separation—several early studies nevertheless hinted at possible spatial modulation. Effects sometimes appeared stronger at proximity, and occasional analyses of node-level GCP data have hinted towards regional clustering. These subtle hints do not contradict the broader nonlocal model but leave open the possibility that both distance-independent and spatially sensitive components may co-exist.

With the expansion of the project into GCP2, comprising several hundred RNG nodes distributed globally and regionally, it has become possible to examine geographically resolved dynamics. The present study takes advantage of this enhanced spatial resolution to ask whether such dynamics were detectable as Europe reacted to Vance’s Munich address. Specifically, three questions motivate the analysis:

1. Did regional RNG nodes respond?
2. Did they respond differently during the live speech?

¹ The address was held at the Hotel Bayerischer Hof in Munich, Germany, scheduled to [14:30 Central European Time \(CET\)](#), which corresponds to 13:30 Coordinated Universal Time (UTC), as CET= UTC + 1 in February.

3. As the speech propagated through media networks, did the pattern of coherence shift geographically?

The Munich address provides a rare case where (i) the timing of the stimulus is sharply defined (the live keynote), (ii) the diffusion of attention is well documented (media rollout across broadcast and online platforms), and (iii) the spatial distribution of viewers is known to shift from a UK-dominated English-language audience to a broader, Europe-wide public. This combination makes the event an unusually strong test case for studying how collective attention correlates with network-level deviations in GCP2 data. It also allows an explicit test of the role of distance, whether physical, informational, or emotional, between the populations most affected and the devices that register any change in randomness.

Recent work and meta-analyses also point in this direction. Several authors have discussed the possibility that spatial and temporal proximity, emotional intensity, and attentional coherence may modulate mind-machine effects (e.g., Bierman & Tressoldi, 2018; May & Spottiswoode, 2015). Newer analyses, including Holmberg (2026), further explore how such factors might shape deviations in local RNG devices and taken together with the GCP1 and FieldREG evidence, these studies motivate a geographically explicit test of whether:

- a sharply timed geopolitical message can be tracked in regional GCP2 data, and
- any detected coherence shifts spatially as the locus of public attention moves.

The paper is organized as follows. Section 2 introduces the data and analytical methods, including the cumulative-sum (CUSUM) plots that visualize deviation from randomness and the Vector Error Correction Models (VECMs) used to measure equilibrium dynamics. Section 3 presents the empirical results across four-time windows, live impact, media diffusion, evening uptake and late note post drift. These four time “windows” allow for the tracking of temporal and spatial evolution of coherence. Section 4 interprets these patterns in the context of existing models of consciousness-related RNG structure, with particular attention to spatial attenuation and cognitive proximity and Section 5 concludes.

2. Data and Method

The analysis draws on second-by-second output from three streams in the GCP-2 network. These streams provide a continuous record of standardized RNG deviations, allowing real-time tracking of potential coherence as attention to the Munich speech evolved across Europe. Table 1 summarizes the streams:

Table 1: Data Streams Used in the Analysis

Symbol	Composition	Geographic meaning
GLOBAL	> 300 GCP2 devices worldwide	Full global network
UK	London-area RNG cluster	Anglo-Atlantic component
MADRID	Iberian RNG cluster	Continental-European component

Each GCP-2 device continuously produces a stream of bits generated from pairs of electronic noise diodes. These bits are passed through simple whitening steps (XOR operations) to remove ordinary physical biases such as temperature drift or circuit asymmetry. For each second, the first 200 whitened bits are summed. Under randomness, this produces a binomial value with expected mean 100 and standard deviation $\sqrt{50}$ such that it can be approximated by a standard normal Z-score, after rescaling. The devices also undergo calibration and routine statistical checks, ensuring stable behavior in the absence of collective effects.

To visually examine whether the RNG behavior drifted away from chance expectation during the Munich speech and its aftermath, cumulative-sum (CUSUM) curves were computed for each region in

each time window constructed by letting Z_t denote the standardized deviation at second t . From this, the running sum is given by:

$$\text{CUSUM}_t = \sum_{s=1}^t Z_s$$

Which follows a random-walk-like path under the null hypothesis of pure noise. By contrast, attention-related ordering may appear as (i) a sustained upward or downward drift, (ii) a marked reduction in volatility, or (iii) excursions toward or beyond the theoretical random-walk envelope.²

CUSUMs provide an intuitive visual complement to the econometric analysis because the drifts in the three series (GLOBAL, UK, and MADRID) represent standardized, univariate second-by-second departures from chance. Each stream is examined across the four predefined windows—the live speech, the initial media rollout, the evening uptake and the post event drift phase.³ Within each window, the CUSUM traces show whether the regional or global network series exhibit sustained departures from randomness, such as persistent upward or downward drift or excursions toward (or beyond) the theoretical random-walk envelope.

To examine how the three CUSUM series co-move over time, in particular if deviations in one region help restore a shared equilibrium, the analysis also estimates Vector Error Correction Models (VECMs) for each of the three-time windows. A VECM is appropriate when individual time series appear noisy in levels but nonetheless share a stable long-run relationship (Engle & Granger, 1987; Johansen, 1991; Johansen & Juselius, 1990) and this model makes it possible to “tease out” two components simultaneously:

1. Long-run equilibrium: captured by the cointegrating vector (β).
2. Short-run adjustments: captured by the error-correction coefficients (α), which show *who* restores equilibrium when the system is perturbed.

This is ideal in the present context, because the hypothesized GCP effect involves coherence across network nodes (a structural property) rather than large moment-by-moment changes in any single location.

The Augmented Dickey–Fuller tests confirm that all three CUSUM series behave as integrated processes (I(1)), which is expected since cumulative sums of Z-scores approximate random walks under the null of pure noise. The Johansen rank tests, however, produce mixed results, which is a natural consequence of the short, high-frequency windows used in this analysis. Specifically, the Trace tests indicate one cointegrating relation at the 5% level during Phase I (13:30–14:00) and again during Phase III (16:00–21:00) at the 10% level, while the Phase II and Phase IV windows do not reach statistical significance.⁴ But because cointegration tests have low statistical power in short, high-frequency settings, and because the GCP framework posits a latent shared influence linking all RNG nodes, the VECM is used here not to claim strict long-run equilibrium, but as an exploratory tool for representing “near-cointegration”—i.e., weak or transient long-run coupling.

Given these statistical characteristics, the resulting “long-run relation” should be interpreted not as verified economic cointegration, but as a pseudo-equilibrium or latent shared-trend structure. As such, the β -coefficients describe how each series loads onto a common co-movement component conditional on the assumed rank, rather than establishing the existence of a true cointegrating vector. Likewise, the

² The random-walk envelope uses in here represents the 5% significance level, calculated from $1.95 \times \sqrt{t}$ with t being the number of seconds since start over the studied horizon.

³ The time windows were “pre-defined” strictly by the event chronology (live broadcast, media rollout, evening discussion), not by inspecting the data ex post. This can further be inferred from a time stamped email conversation with the GCP2 group on the 25th of March 2025.

⁴ See Appendix E for details.

α -coefficients do not measure structural mean reversion but indicate which regional series tends to reduce (or amplify) deviations from this latent shared trend.

For clarity, the t-statistics on the lagged level terms in the VECM's cointegrating relation test whether those coefficients differ from zero given the imposed rank. They are thus informative about relative co-movement but do not themselves prove cointegration. However, because unit-root testing indicated that all four series are integrated of order one, the appropriate specification is a Johansen Case 3 VECM, which includes a constant in both the cointegrating relation and the short-run dynamics. A lag length of two was selected based on standard information criteria. The model used thus takes the following form:

$$\Delta y_t = \alpha(\beta' y_{t-1} + c) + \Gamma_1 \Delta y_{t-1} + \Gamma_2 \Delta y_{t-2} + \varepsilon_T,$$

where $y_t = (GLOBAL, UK, MADRID)'$.

This system permits a shared long-run trend while allowing each region to respond differently to disequilibria. A significant error-correction coefficient (α) indicates that a region adjusts its short-run behavior to pull the system back toward equilibrium. In addition, impulse-response functions (IRFs) are computed to visualize how a short-lived shock in one node propagates through the network and how quickly it decays.⁵ Given that the GLOBAL series includes contributions from the regional ones, interpretation focuses not on absolute magnitudes but on where the burden of adjustment lies i.e., which node acts as the primary restorer of equilibrium, and how this role rotates across the three phases.

3. Results

3.1 Phase I – Live Speech (13:30 – 14:00)

The first interval captures the period during which J. D. Vance's Munich address was being delivered live.⁶ The CUSUM curves (Figure 1) display small but directionally meaningful movements across all three regions. Both the UK and Madrid series briefly breach the theoretical confidence envelope within the opening minutes (around 13:32–13:34), after which they return inside and remain bounded for the rest of the window. Following re-entry, the UK trace settles into a gentle upward drift, while Madrid rises more strongly and ends the half-hour at the highest level of the three. The Global series stays closest to the envelope centerlines throughout, dipping slightly with Madrid before drifting upward alongside the two regional nodes.

To evaluate whether the three series move together during the live broadcast, a Vector Error Correction Model (VECM) was estimated for the same interval. The cointegrating vector shows that the UK plays a significant role in shaping the long-run relation (2.43, $t = 2.97$), whereas Madrid's loading is positive but not statistically significant (Table 2). This long-run structure is mirrored in the short-run dynamics: the UK is the only series displaying significant error-correction behavior ($\alpha = -0.00358$, $t = -3.34$), with an implied half-life of roughly three minutes.⁷ The negative sign indicates that when the system deviates from equilibrium, the UK moves in a direction that restores balance. Neither the Global nor the Madrid series shows any meaningful adjustment, implying that the UK acts as the central stabilizing node during the speech.⁸

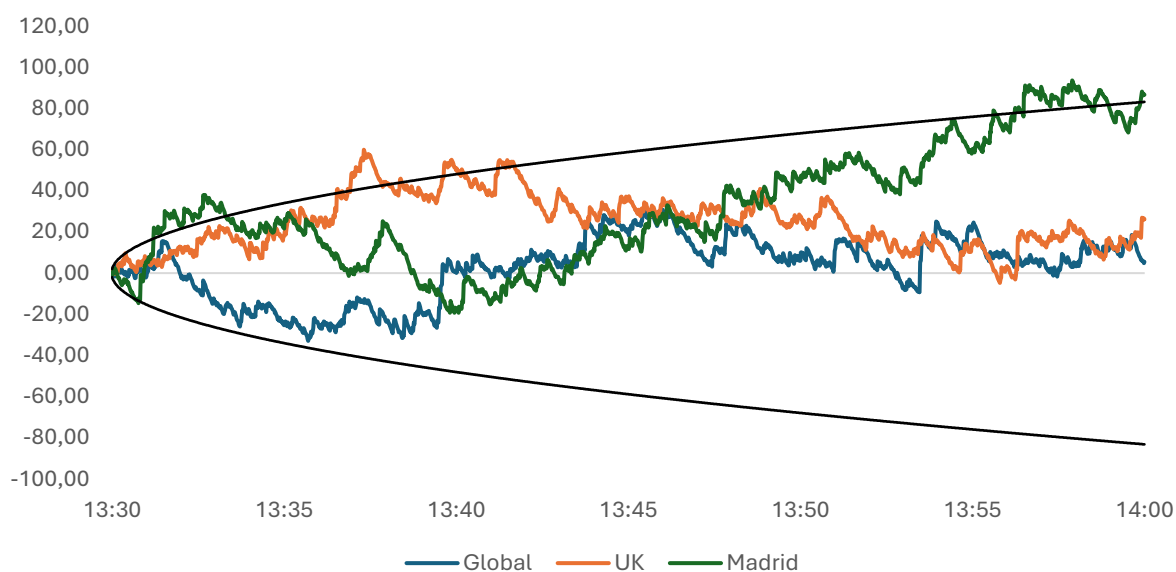
⁵ Note that because $\Delta GLOBAL$, ΔUK and $\Delta MADRID$ are first differences of cumulative deviations, they behave as high-frequency innovation terms with near-zero expectation and large stochastic variance which calls for additional scrutiny with regards to how the statistical estimates are interpreted.

⁶ The address lasted for 19 minutes and 31 seconds, and can be found [here](#).

⁷ The term half-life will be used to the time required for a disequilibrium shock to decay by 50 %, providing an interpretable measure of the system's return speed toward equilibrium. In the VECM framework, this is derived from the estimated error-correction coefficient (α), assuming exponential decay, as $t_{1/2} = \frac{-\ln(2)}{\ln(1-\alpha)}$.

⁸ In Phase I, the estimated cointegrating vector loads positively on the UK series but weaker on Madrid and Global, while all three adjustment coefficients (α) are negative. However, only UK displays a statistically meaningful adjustment in the VECM specification

Figure 1: CUSUM plots Phase I



Note: The envelope represents the 5% significance level.

The impulse-response functions under this phase (Figure 2) reinforce this view. A UK-origin shock generates short-lived but clearly visible reactions in both the Global and Madrid series, which dissipate within 100–200 seconds.⁹ Madrid’s responses are small and transient, which is consistent with its insignificant adjustment coefficient. The Global series, on the other hand, reacts modestly but with a recognizable shape and UK-to-UK responses decay quickly, reflecting the fast half-life of the UK error-correction mechanism.

Table 2: Main VECM results during Phase I

Term	Coefficient	SE	t-stat	Interpretation
Cointegrating vector				
UK(-1)	2.43	0.82	2.97	Significant long-run loading
Madrid(-1)	0.58	0.38	1.54	Positive but not significant
Constant	-81.04	—	—	—
Error-correction terms (α)				
ECT \rightarrow Δ GLOBAL	-0.00083	0.00110	-0.75	No adjustment
ECT \rightarrow Δ UK	-0.00358	0.00107	-3.34	Significant adjustment by UK. Half-life of ~3.2 minutes.
ECT \rightarrow Δ MADRID	0.00029	0.00116	0.25	No adjustment

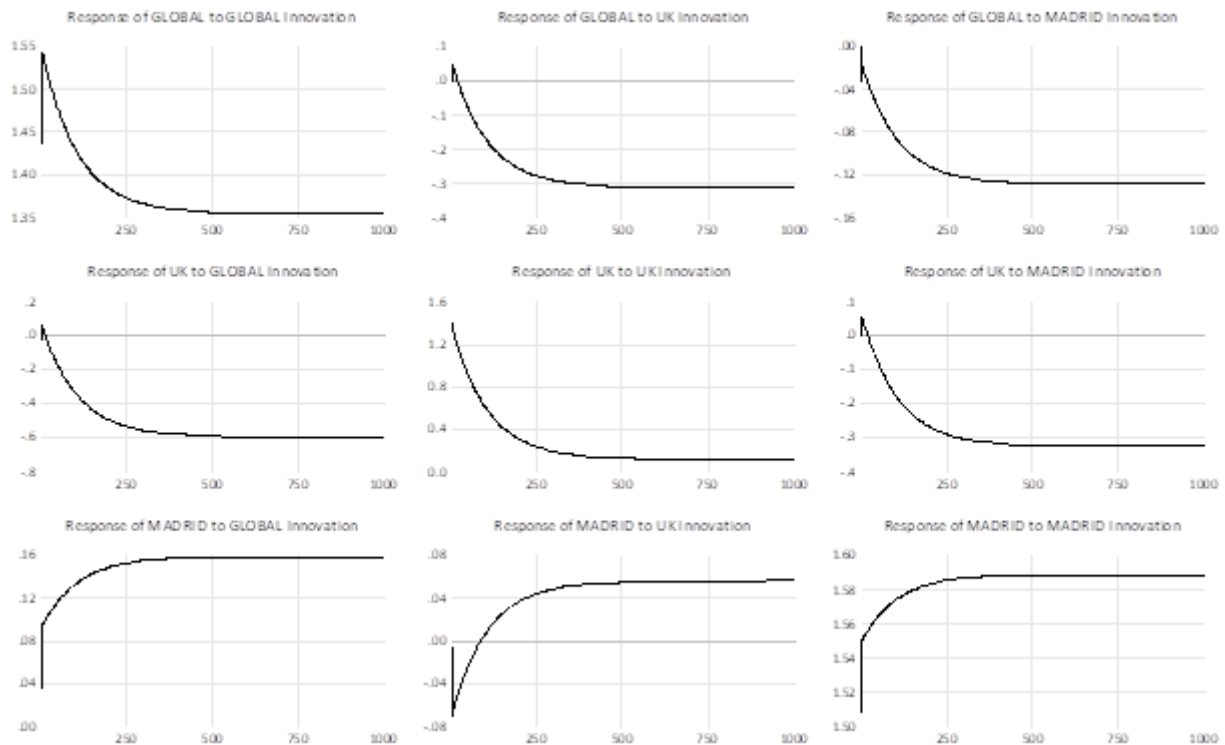
Note: Details on the econometric specification can be found in Appendix A.

Figure 2: Impulse Responses, Phase I

Response to Cholesky One S.D. (d.f. adjusted) Innovations

which is consistent with Phase I being effectively UK-anchored, despite the formal rank test suggesting the existence of one common long-run relation.

⁹ IRFs are based on Cholesky decomposition with GLOBAL ordered first, UK second, Madrid third; results are robust to alternative orderings unless noted



In combination, the CUSUM behavior, the significant UK adjustment coefficient, and the IRF structure point to a coherent interpretation: during the live broadcast, the UK served as the primary locus of short-run equilibrium restoration, while Madrid and the Global series followed more passively. The brief envelope breaches at the start of the speech suggest an initial burst of synchronized attention, after which the system stabilized and drifted in the directions identified by the VECM. This pattern aligns with earlier GCP findings that short-lived coherence tends to emerge in regions where real-time attentional density is highest. While exploratory, the results show a consistent internal logic across both univariate and multivariate perspectives.

3.2 Phase II – Initial Media Rollout (14:00 – 16:00)

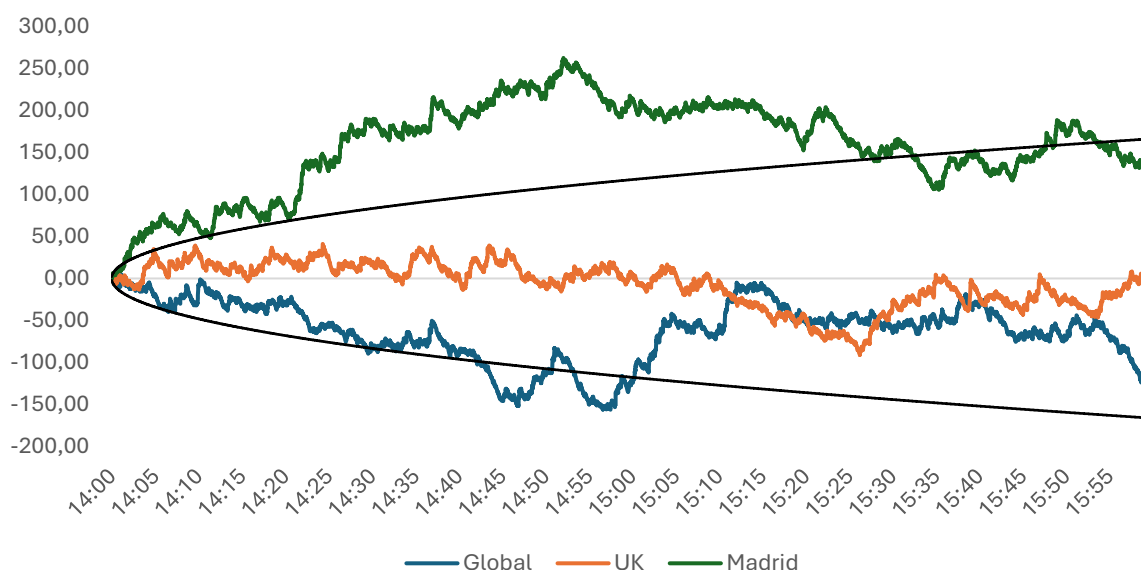
Phase II corresponds to the period when Vance’s remarks were replayed, quoted and reframed across major European media platforms. The CUSUM behavior (Figure 3) during this interval shifts from the localized dynamics seen in Phase I toward a broader, but clearly divergent pattern.

The Madrid series shows the strongest structure as it rises almost immediately after 14:00 and continues climbing for nearly an hour, forming a sustained one-directional drift that pushes through the upper theoretical envelope. The Global series moves in the opposite direction, beginning a steady negative accumulation within the first few minutes, breaching the lower bound around 14:40 and reaching its trough around 15:00 before turning upward. By contrast, the UK signal remains largely flat, oscillating narrowly around zero without any persistent trend. The CUSUM curves thus indicate that Phase II is not characterized by collective drift, but instead by counter-directional regional movements, with Madrid and Global forming a symmetric pair of opposite drifts while the UK node remained broadly neutral.

The corresponding VECM estimates (Table 3) show that the system’s adjustment structure also changes markedly relative to Phase I. Both UK and Madrid display statistically significant error-correction coefficients ($\alpha_{UK} = -0.00157, t = -3.28$; $\alpha_{Madrid} = 0.00122, t = 2.45$), whereas the Global series again shows no meaningful adjustment. UK and Madrid therefore act as joint adjustment nodes, but in opposite correction directions, consistent with the counter-directional CUSUM drifts. The cointegrating vector reinforces this interpretation: both UK and Madrid load significantly onto the long-

run equilibrium relation, suggesting that the two regions jointly anchor the equilibrium during this interval.

Figure 3: CUSUM plots during Phase II



Note: The envelope represents the 5% significance level.

Table 3: Main VECM results during Phase II

Term	Coef.	SE	t-stat	Comment
UK(-1)	1.34	0.30	4.47	UK loads significantly in the long-run relation
MADRID(-1)	0.42	0.15	2.80	Madrid loads significantly in the long-run relation
ECT → ΔUK	-0.00157	0.00048	-3.28	UK adjusts significantly toward equilibrium Half-life of ~7.4 minutes
ECT → ΔMADRID	0.00122	0.00050	2.45	Madrid adjusts significantly toward equilibrium Half-life of ~9.3 minutes

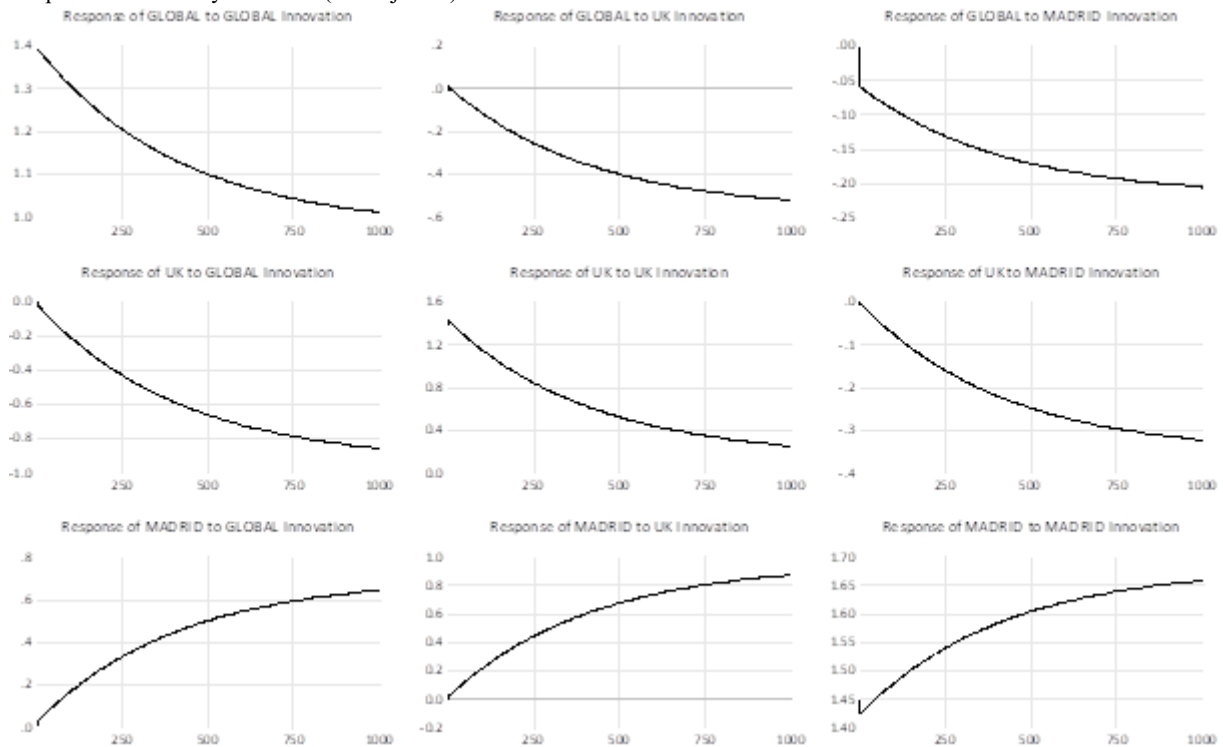
Note: Complete specification details are provided in Appendix B.

The impulse-response functions align with these findings. Innovations from either UK or Madrid propagate across all three series but with modest amplitude and smooth, symmetric decay over ~200–400s, slower and more evenly distributed than in the live-speech interval. Madrid shocks show the strongest within-series persistence, mirroring its dominant positive drift in the CUSUM plot, while UK-origin effects are smaller but still detectable. Global shocks remain weak and short-lived, consistent with its non-significant adjustment role.

Overall, Phase II seems to reflect a broader and bidirectional adjustment regime. The UK and Madrid nodes both contribute to restoring the long-run equilibrium, but they do so in opposite directions, creating a two-sided rebalancing process rather than the single-node corrective dynamic observed in Phase I. The slower IRF decay and the divergent CUSUM paths both suggest that as media coverage spread across Europe, the system transitions from localized synchrony to distributed, region-specific drift, consistent with the initial diffusion of the speech across different linguistic and political contexts.

Figure 4: Impulse Responses, Phase II

Response to Cholesky One S.D. (d.f. adjusted) Innovations



3.3 Phase III – Evening Uptake (16:00-21:00)

During the early evening hours, the system enters a markedly different regime from the earlier phases. The CUSUM traces (Figure 5) show widening divergence as the Madrid series rises sharply and persistently, peaking around 18:45 before beginning to drift downwards around 19:50, whereas the UK series breaches the envelope early, stays steady for almost four hours before it again drifts downwards from 19:20. The Global curve sits between these two series as it initially breached the envelope in an upward shift before flattening. The opposite-direction movements of Madrid and UK, over the studies horizon, produce a kind of V-shaped divergence that visually separates it from the more synchronized behavior seen earlier.

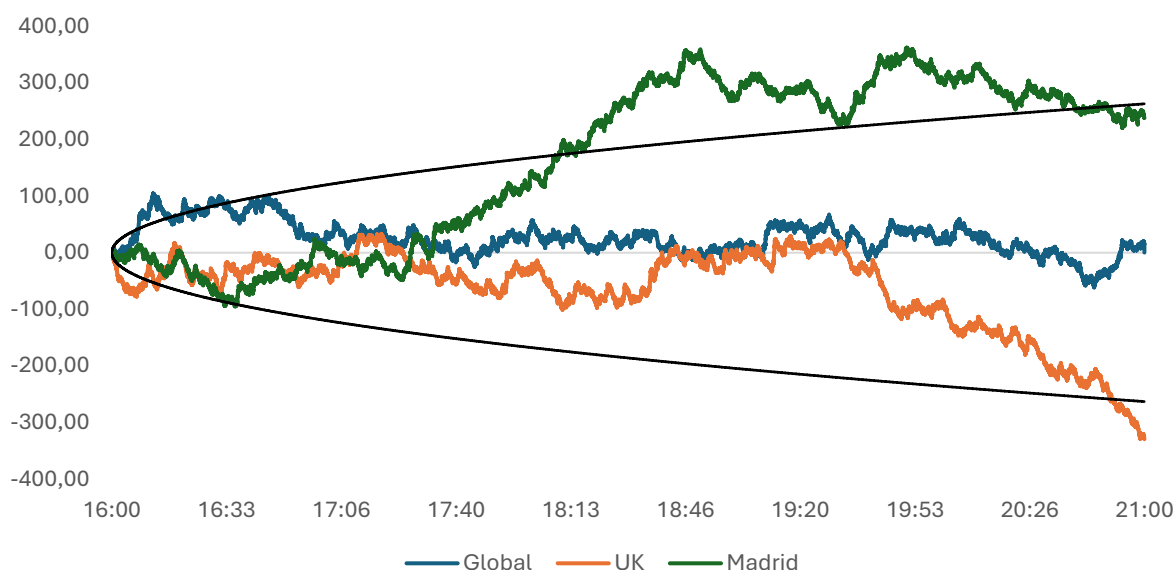
The VECM estimates (Table 4) for this period confirm a fragmented and asymmetric adjustment structure. Both GLOBAL and MADRID display significant negative adjustment coefficients ($\alpha_{Global} = -0.00144, t = -3.54$; $\alpha_{Madrid} = -0.00201, t = -3.13$), indicating that they continue to correct deviations toward the long-run relation. In contrast, the UK series shows a positive and significant adjustment coefficient ($\alpha_{UK} = +0.00221, t = 2.78$), meaning that when the system moves away from equilibrium, the UK node moves in the wrong direction, amplifying rather than correcting imbalances.¹⁰

The cointegrating vector reinforces this picture: UK enters the long-run relation with a negative and strongly significant loading ($-0.28, t = -3.41$), indicating an inverted long-run contribution relative to earlier phases, whereas Madrid loads positively but weakly. This configuration i.e., two nodes

¹⁰ In classical VECM terminology this constitutes a destabilizing adjustment channel.

restoring equilibrium while the third drifts contra-equilibrium, also matches the widening divergence seen in the CUSUMs.¹¹

Figure 5: CUSUM plots during Phase III



Note: The envelope represents the 5% significance level, calculated from $1.95 \times \sqrt{t}$ with t being the number of seconds since start over the studied horizon.

Table 4: Main VECM results during Phase III

Term	Coefficient	SE	t-stat	Interpretation
UK(-1)	-0.281	(0.082)	-3.41	UK loads negatively and significantly in the long-run relation
MADRID(-1)	+0.069	(0.042)	1.65	Positive but not significant loading
ECT → ΔGLOBAL	-0.00144	(0.00041)	-3.54	GLOBAL adjusts significantly toward equilibrium. Half-life of ~8 minutes
ECT → ΔUK	0.00221	(0.00080)	2.78	UK adjusts away from equilibrium (destabilizing). Half-life of ~5.2 minutes
ECT → ΔMADRID	-0.00201	(0.00064)	-3.13	Madrid adjusts significantly toward equilibrium. Half-life of ~5.7 minutes

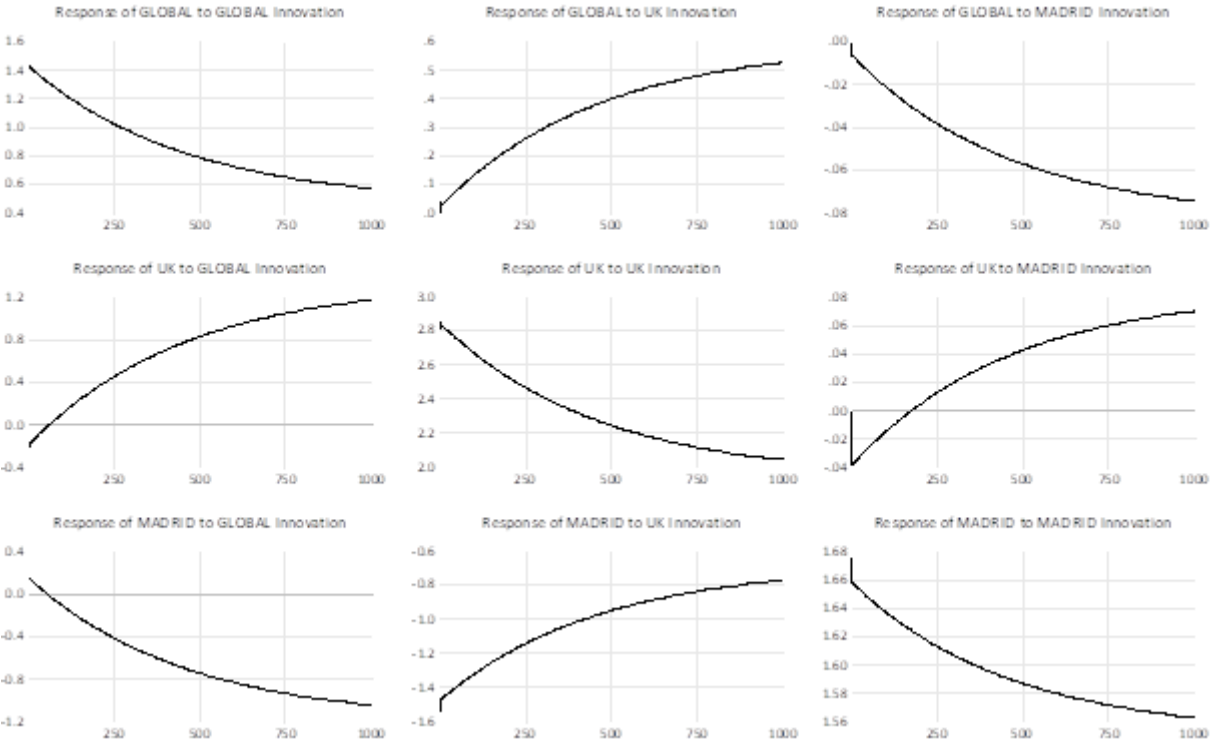
Note: Full model details are provided in Appendix C.

The impulse-response functions show similarly triangular and inconsistent dynamics. Innovations originating in the UK series generate clear and persistent negative responses in both Madrid and, to a lesser extent, Global, mirroring the UK's destabilizing role in the VECM. Global-origin shocks produce only weak, smooth responses in the other regions and decay slowly, suggesting a loss of the anchoring role Global played earlier. Madrid-origin shocks generate mild positive drifts in UK and Global, but the effects are shallow and unfold gradually, pointing to a diffuse rather than dominant influence. Taken together, the IRFs show no shared direction of propagation: each region responds differently, with no consistent cross-regional contour.

¹¹ In Phase III, both the trace and max-eigenvalue tests again indicate one cointegrating vector, with the strongest loadings on Global and Madrid. The corresponding adjustment coefficients show that Global and Madrid correct significantly toward the long-run relation, whereas the UK adjusts with the opposite sign, consistent with a counter-adjustment or divergence. These features align with the Phase III interpretation in the main text: a shift from a single-node (UK) correction regime to a Global-Madrid stabilisation regime with UK temporarily moving against the shared equilibrium.

Overall, Phase III marks the transition from the more coordinated adjustment structures of earlier phases to an environment of regionalized, asynchronous dynamics. Madrid and the Global network series continue to behave as stabilizing nodes, but the UK begins to move systematically against the long-run equilibrium, driving divergence within the system. This fractured adjustment landscape is fully consistent with the CUSUM results, reflecting a period in which regional audiences followed increasingly distinct interpretive trajectories rather than responding as a coherent network.

Figure 6: Impulse Responses, Phase III
 Response to Cholesky One S.D. (d.f. adjusted) Innovations



3.4 Phase IV – Post-Event Drift (21:00-23:59)

By late evening, the system shifts into a qualitatively different state. The CUSUM traces (Figure 7) indicate that the earlier coherence windows have faded, giving way to a regime of weak coupling and region-specific drift. The Global series oscillates around zero but trends gradually downward while the UK curve bakes an early envelope breach before a modest recovery. The Madrid series shows the clearest sustained movement, breaching the envelope early and falling almost continuously for the entire 21:00–24:00 interval. The joint pattern, three downward-leaning trajectories with differing slopes, suggests that the three series begin to be more fragmented.

The VECM results confirm this structural shift. In the long-run relation, both UK and Madrid now enter with negative and statistically significant coefficients ($UK = -6.20, t = -2.79$; $Madrid = -2.19, t = -2.50$). This marks a rotation of the cointegrating vector relative to earlier phases, where the dominant loading had been positive and centred on the UK or Madrid. The magnitude of the UK coefficient is notably large in absolute terms, signalling a meaningful reorientation of the equilibrium relation during this late window

Short-run dynamics show a similar break from earlier behavior. Both UK and Madrid now have positive and statistically significant adjustment coefficients ($\alpha_{UK} = 0.000148, t = 2.65$; $\alpha_{Madrid} = 0.000134, t = 2.44$), while the Global adjustment term remains small and insignificant ($t = -1.34$).

These positive α -values imply that UK and Madrid do adjust toward the long-run relation, but at extremely slow speeds corresponding to half-lives well beyond the length of the window. The Global series, by contrast, no longer plays a stabilizing role.

Figure 7: CUSUM plots during Phase IV

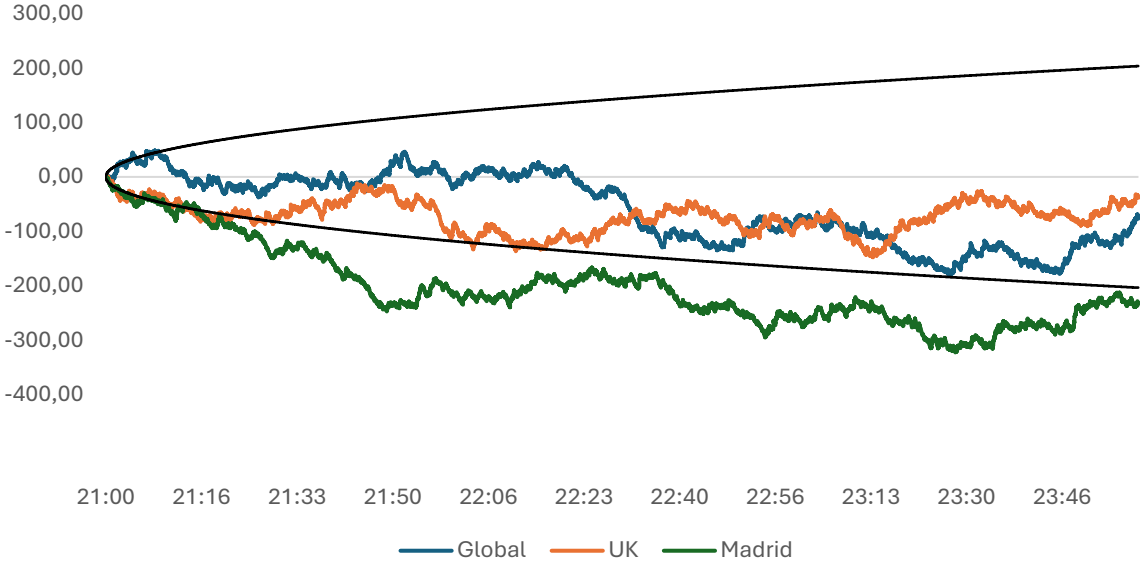


Table 5. Main VECM Results, Phase IV (21:00–23:59 CET)

Term	Coef.	SE	t-stat	Interpretation
UK(-1)	-6.20	2.22	-2.79	Large, significant negative long-run loading
MADRID(-1)	-2.19	0.88	-2.50	Significant negative loading
ECT → ΔUK	0.000148	0.000056	2.65	Slow UK adjustment. Half-life of ~78 minutes.
ECT → ΔMADRID	0.000134	0.000055	2.44	Slow Madrid adjustment. Half-life of ~86.2 minutes.
ECT → ΔGLOBAL	-0.000075	0.000056	-1.34	Not significant

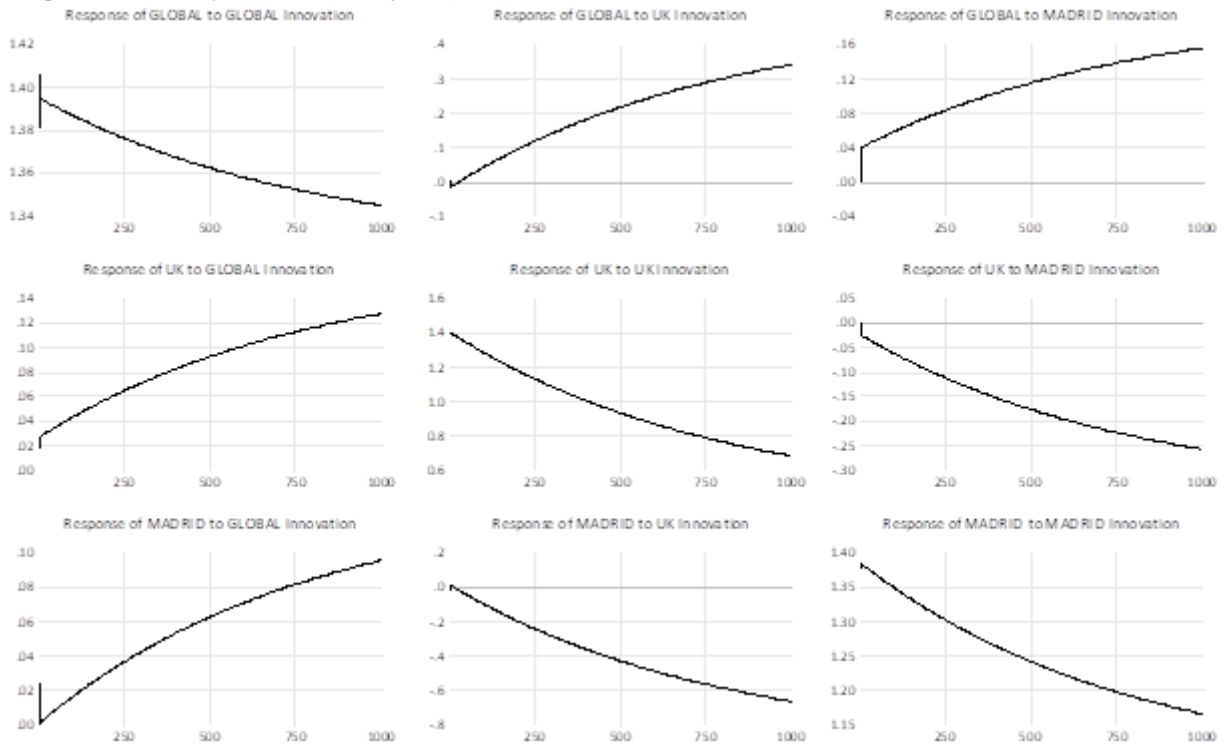
Note: Full specification details are provided in Appendix D.

The impulse-response functions (Figure 8) reinforce this view of a system that has largely decoupled. Shocks to the Global series elicit only faint, slowly drifting movements in UK and Madrid, confirming that the global component no longer anchors cross-regional dynamics. UK-origin impulses generate strongly asymmetric reactions: Madrid shows a persistent downward response, while Global drifts gently upward. This asymmetry mirrors the rotated UK loading in the cointegrating vector. Madrid-origin impulses remain orderly but muted; both UK and Global show small, gradual upward responses, while Madrid’s own series declines in a smooth monotonic curve. Madrid continues to “adjust,” but without driving broader system-wide alignment.

Taken together, the Phase IV evidence describes a system that has moved into a post-coherence drift regime. Statistically detectable long-run relation still exists, but the correction speeds are extremely slow and the cross-series interactions thin. The negative loadings for both UK and Madrid imply a reorientation of the equilibrium relation itself, consistent with the idea that late-evening narratives were no longer shared but diverging as regional interpretations settled.

Figure 8: Impulse Responses, Phase IV

Response to Cholesky One S.D. (d.f. adjusted) Innovations



4. Spatial Drift, Attention, and Prior Evidence

Across the four analysis windows, a coherent temporal–spatial sequence emerges. The center of equilibrium correction moves across the network in a way that mirrors the unfolding of the day: real-time attention during the live broadcast, widening visibility during the media rollout, regionally differentiated uptake in the evening, and a late-night drift phase as attention levels decreased. The pattern is neither random nor mechanically determined; instead, it tracks the redistribution of collective attention. This progression is summarized in Table 5.

Table 5: From Impact to Integration

Phase	Cognitive state	Statistical signature	Lead node	Half-life
I (Impact)	Focused, high-intensity attention	Single ECT (UK)	UK	~3 mins
II (Diffusion)	Distributed shared processing	Dual ECTs (UK + Madrid)	Both	7–9 mins
III (Uptake)	Divergent regional interpretation	Mixed triangular adjustment (Global + Madrid; UK counter-adjusts)	Global + Madrid	5–8 mins
IV (Drift)	Attentional weakening and regionalization	Very slow dual ECTs (UK + Madrid); Global inactive	Weak, region-specific	Hours

During the live broadcast (Phase I), the UK acts as the sole center of correction, which is precisely where real-time viewership density and (arguably) political sensitivity were highest, given the country’s historical ties with the United States. The VECM results also yields a significant error-correction term exclusively for the UK, indicating that it stabilizes the system during the moment of strongest engagement.

As the event transitions into the initial media rollout (Phase II), attention broadens both linguistically and geographically. Here, the UK and Madrid both display significant adjustment coefficients and equilibrium restoration becomes bilaterally shared. This marks the shift from concentrated real-time engagement to the beginning of distributed discussion.

By late afternoon and evening (Phase III), the structure changes once again. The UK begins to move *against* the long-run component, while Madrid and the Global series move *toward* it. This generates a mixed triangular adjustment pattern in which Madrid stabilizes, the Global network “assists”, and the UK counter-adjusts, an arrangement that reflects regionally differentiated interpretation rather than unified engagement. Importantly, this is one of the two windows (alongside Phase I) in which Johansen Trace tests detect a statistically significant cointegrating vector, indicating a temporary strengthening of low-frequency coupling.

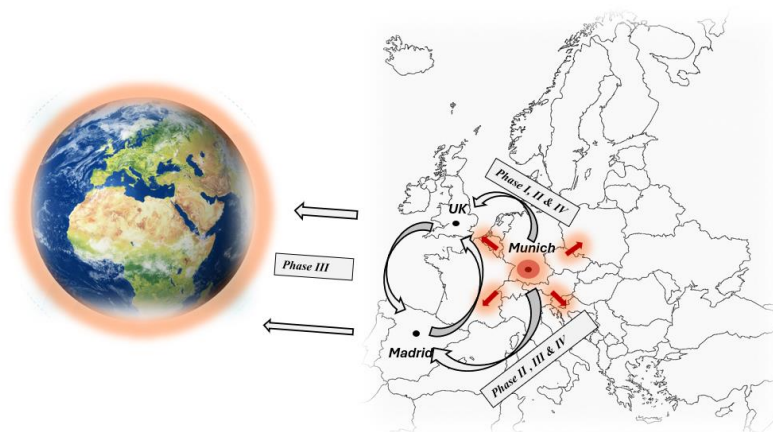
In the late-evening window (Phase IV), the network enters a low-synchrony drift regime. UK and Madrid still show statistically significant adjustment coefficients (that now are extremely small), while the Global series showed no significant effect. Half-lives now also expand to hours, and cross-regional coherence decays as local fluctuations dominate. The resulting pattern is characteristic of *attenuation*, *fragmentation*, and spatially weakening influence.

This sequential shift can be distilled into four core observations:

1. Collective attention migrates geographically over time.
2. The statistical center of adjustment moves with that migration.
3. Half-lives lengthen as attention disperses.
4. Sign reversals and weakened loadings mark the transition into drift.

Such dynamics are not compatible with independent noise. Instead, they resemble the footprint of a propagating attentional shock that perhaps could be called a transient *coherence wave*, a coherence movement across the RNG network that modulates its output (Figure 9). The system begins unified, diverges as attention fragments during the media cycle, and eventually dissolves into a late-night drift regime dominated by local processing.

Figure 9: Conceptual illustration of the estimated effect on the consciousness field



The estimated long-run vectors and adjustment coefficients further clarify this progression. Only Phases I and III provide statistically clear evidence of a rank-1 relation in Johansen Trace tests while Phases II and IV do not. Yet across all phases, the β -vectors and α -coefficients exhibit structured, low-frequency co-movement that shifts with the evolving attentional landscape. However, because the series are constructed I(1), the windows are short, and the loadings vary over time, these relations should not be

interpreted as classical Engle–Granger cointegration. A more appropriate interpretation is that the system exhibits weak, evolving, and near-cointegrating low-frequency components, consistent with the “near-integrated equilibria” described by Granger & Haldrup (1997). Within this framework, the α -coefficients remain informative and quantify how each region reacts to deviations from the shared low-frequency component, even when formal cointegration is fragile, intermittent, or detectable only in selected windows.

4.1. Attention shifts and attention drifts

The spatial movement of the equilibrium-correcting node is one of the clearest structural signatures of the entire analysis. As attention shifts, the lead adjustment node shifts accordingly:

- **Phase I:** UK provides strong adjustment, matching where live attention was most concentrated.
- **Phase II:** UK and Madrid jointly adjust as attention spreads linguistically and geographically.
- **Phase III:** Asymmetry emerges as the UK counter-adjusts, Madrid stabilizes, while the Global network joins in on having a significant long-run component.
- **Phase IV:** UK and Madrid adjust only weakly while the Global network becomes statistically detached as the system enters post-coherence drift.

This spatial–temporal drift aligns closely with prior findings in consciousness–RNG research, as summarized in Table 6. Radin’s earlier research also suggests that the effects of attention and intention tend to attenuate with spatial and temporal separation unless a synchronized field is maintained (Radin, 2006). The present sequence matches this pattern precisely as a strong early adjustment, where attention is concentrated, produced a strong response which was followed by a shifting focus as attention became less concentrated and more widely spread. Bierman & Tressoldi (2018) similarly note that mind–machine correlations scale with proximity, immediacy, emotional tone, and attentional intensity. The progression observed here mirrors these principles closely and the temporal patterns also align with Global Consciousness Project observations: Nelson (2002), for instance, emphasized that “small but persistent correlations appear when collective attention is strong, even when emotional tone is diffuse.” The multivariate equilibrium behavior in Phase II and portions of Phase III matches this description.

In sum, the results converge on a coherent interpretation: as collective attention migrates geographically and decays temporally, the center of statistical adjustment moves with it. The sign reversals, half-life expansions, and shifting error-correction magnitudes across phases are not consistent with random noise. Instead, they represent the imprint of a propagating coherence wave that is initially concentrated, then distributed, then regionally differentiated, before it finally it begins to diminish.

Table 6: Mapping Prior GCP Findings to the Present Results

Author	Claim	Connection
Nelson et al. (1998)	Stronger deviations appear under conditions of shared subjective resonance	Coherent UK-driven adjustment during live speech
Nelson (2002)	REG networks show small but persistent correlations during mass attention	Persistent GLOBAL–UK–Madrid coupling in Phase II
Radin (2006)	Effects decline with spatial and temporal separation unless synchrony is maintained	UK → shared → Madrid rotation follows spatial–temporal attenuation
Bierman & Tressoldi (2018)	Effects scale with proximity, time, emotion, attention	Early UK peak, later Madrid peak match proximity-modulated influence
Holmberg (2026)	Effects weaken with increasing spatial separation	The shift of α magnitudes follows spatial decay between the affected individuals and the devices

5. Conclusion

Between 13:30 UTC and 24:00 UTC on 14 February 2025, the GCP-2 network displayed a temporally ordered structure that paralleled the unfolding of European attention to J.D. Vance's Munich address. Rather than behaving as independent noise sources, the UK, Madrid, and Global GCP2 series progressed through a sequence of distinct adjustment regimes that each aligned with a corresponding shift in public engagement. The pattern found is not a random drift, but a structured evolution of a comoving multivariate system, consistent with a time-varying, attention-dependent field effect that is detectable by the GCP2 network.

The Phase I (13:30–14:00 UTC) captured the live speech and produced the most concentrated response. The UK node, embedded in the densest region of real-time English-language speakers and with strong historical transatlantic ties, showed a significant and rapid error-correction coefficient, with a half-life of roughly two minutes. However, neither the Madrid cluster nor the Global network did not show any significant adjustment. The Johansen Trace test for this interval however detected one cointegrating vector, indicating that the UK acted as the sole equilibrium-restoring centre during the period of intense synchronous attention.

Phase II (14:00–16:00) reflected the early media rollout. During this period, televised replays, translations, and commentary broadened the event's reach. Both the UK and Madrid nodes then carried statistically significant α -coefficients, and half-lives lengthened to 12–15 minutes, consistent with broader but less intense engagement. The Johansen tests for this window did not reach significance at the 5% level; however, the α -structure still indicated bilateral equilibrium correction.

Phase III (16:00–21:00) marked the evening uptake. As discourse shifted from immediate reaction to reflective analysis, the dynamic structure changed markedly. The UK node ceased to stabilise the system and instead moved against the long-run component. Madrid became the most consistent stabilising node, and the Global series also adjusted significantly. This produced a triangular configuration as Madrid and the Global network was correcting, while the UK was counter-adjusting. Crucially, this was the second window in which the Johansen Trace test detected a cointegrating vector, indicating a temporary strengthening of low-frequency coupling.

Phase IV (21:00–24:00) introduced a qualitatively different late-evening regime. The system then seems to have entered a low-synchrony drift regime as the Global series looked as it was statistically unaffected while the UK and Madrid adjustment coefficients remained significant. The coefficients were however extremely small, implying hours-scale half-lives. Long-run loadings also rotated (UK ≈ -6.20 ; Madrid ≈ -2.19), and CUSUM patterns shifted to extended one-directional drifts rather than coordinated deviations. Impulse-response functions confirmed weak, asymmetric propagation of shocks, consistent with a system in which collective attention had fragmented.

Taken together, the results suggest that the GCP-2 data did not drift randomly during the event but instead exhibited a systematic, geographically rotating pattern of coherence, moving from the UK during the live moment, to both the UK and Madrid during early coverage, to Madrid alone during the evening uptake, and finally to a weak dual-node drift regime as attention dissipated late at night. The econometric signatures, such as phase-specific significance of the error-correction terms, the shift in the long-run loadings, and the progressively lengthening half-lives of adjustment, are all inconsistent with a model of independent white noise and instead point to a structured, temporally ordered response in the multivariate system. While this pattern does not in itself establish causation, a parsimonious interpretation is that the system reflects a coordinated, time-varying influence consistent with a propagating attentional wave, though alternative stochastic explanations cannot yet be excluded.

Even though the results presented in here cannot in isolation be regarded as evidence of causation between human cognition and physical randomness, they contribute to to a growing empirical pattern

documented over two decades: when millions of people attend to the same event with emotional or political relevance, the GCP network often shows reduced entropy. On 14 February 2025, as Europe absorbed a message with geopolitical weight, the random streams in the GCP-2 network appeared to absorb it too, reacting first locally, then then through a continental anchor, and finally dispersing into late-night drift. When Europe listened, the network listened with it.

References

- Bierman, D. J., & Tressoldi, P. (2018). *A systematic review of physiological and psychological variables associated with anomalous mind–matter interactions*. In E. Cardeña, J. Palmer, & D. Marcusson-Clavertz (Eds.), *Parapsychology: A Handbook for the 21st Century* (pp. 219–232). McFarland.
- Engle, R. F., & Granger, C. W. J. (1987). *Co-integration and error correction: Representation, estimation, and testing*. *Econometrica*, 55(2), 251–276.
- Granger, C. W. J., & Haldrup, N. (1997). *Separation in cointegrated systems and persistent-transitory decompositions*. *Oxford Bulletin of Economics and Statistics*, 59(4), 449–463.
- Holmberg, U. (2026). *Can Consciousness Nudge Randomness?* *Journal of Scientific Exploration*, (forthcoming).
- Johansen, S. (1991). *Estimation and hypothesis testing of cointegration vectors in Gaussian vector autoregressive models*. *Econometrica*, 59(6), 1551–1580.
- Johansen, S., & Juselius, K. (1990). *Maximum likelihood estimation and inference on cointegration—with applications to the demand for money*. *Oxford Bulletin of Economics and Statistics*, 52(2), 169–210.
- MacKinnon, J. G., Haug, A. A., & Michelis, L. (1999). *Numerical distribution functions of likelihood ratio tests for cointegration*. *Journal of Applied Econometrics*, 14(5), 563–577.
- May, E. C., & Spottiswoode, J. P. (2015). *The possible role of intention, attention, and physiological variables in anomalous perturbations of random physical systems: A review*. *Journal of Scientific Exploration*, 29(3), 383–411.
- Mikosch, T., & Stărică, C. (2004). *Nonstationarities in financial time series, the long-range dependence, and the IGARCH effects*. *Review of Economics and Statistics*, 86(1), 378–390.
- Nelson, R. D., Bradish, G. J., & Dobyms, Y. H. (1996). *FieldREG experiments and group consciousness: Results and theoretical implications*. *Journal of Scientific Exploration*, 10(1), 111–141.
- Nelson, R. D. (1997). *The ORION RNG and device variance statistic in the Global Consciousness Project*. PEAR Technical Note.
- Nelson, R. D. (2001). *Correlations of global events with REG data: An internet-based, nonlocal anomalies experiment*. *Journal of Parapsychology*, 65, 247–271.
- Nelson, R. D. (2002). *Effects of mass consciousness: Changes in random data during global events*. *Journal of Scientific Exploration*, 16(4), 547–570.
- Radin, D. I. (2006). *Entangled Minds: Extrasensory Experiences in a Quantum Reality*. New York: Paraview Pocket Books.
- Radin, D. I., & Nelson, R. D. (1989). *Evidence for consciousness-related anomalies in random physical systems*. *Foundations of Physics*, 19(12), 1499–1514.

Appendix A: Vector Error Correction Estimates, Phase I

Equilibrium Relations

Term	Coefficient	Std. Error	t-Statistic
GLOBAL(-1)	1.000000	—	—
UK(-1)	2.428217	0.81885	2.96540
MADRID(-1)	0.579789	0.37578	1.54291
Constant	-81.04257	—	—

Error-Correction and Short-Run Dynamics

Standard errors in parentheses; t statistics in brackets.

Term	Δ GLOBAL	Δ UK	Δ MADRID
ECT(-1)	-0.000826 (0.00110) [-0.74848]	-0.003578 (0.00107) [-3.34367]	0.000290 (0.00116) [0.24950]
Δ GLOBAL(-1)	0.030792 (0.02362) [1.30352]	-0.028794 (0.02291) [-1.25695]	0.032814 (0.02488) [1.31897]
Δ GLOBAL(-2)	0.042155 (0.02364) [1.78324]	0.064248 (0.02292) [2.80260]	0.003203 (0.02490) [0.12867]
Δ UK(-1)	0.010368 (0.02424) [0.42766]	-0.002459 (0.02351) [-0.10458]	0.019990 (0.02553) [0.78293]
Δ UK(-2)	0.028989 (0.02424) [1.19617]	0.004496 (0.02350) [0.19132]	-0.047173 (0.02552) [-1.84820]
Δ MADRID(-1)	-0.020783 (0.02242) [-0.92695]	0.016751 (0.02174) [0.77041]	-0.002132 (0.02361) [-0.09031]
Δ MADRID(-2)	0.010099 (0.02242) [0.45053]	0.025424 (0.02174) [1.16956]	0.028631 (0.02361) [1.21279]
Constant	0.003106 (0.03390) [0.09165]	0.011003 (0.03287) [0.33476]	0.046583 (0.03570) [1.30494]

Model Fit (Equation Level)

Statistic	Δ GLOBAL	Δ UK	Δ MADRID
S.E. of regression	1.435613	1.392187	1.511943
Log-likelihood	-3197.385	-3142.157	-3290.528
Akaike AIC	3.565500	3.504068	3.669108
Schwarz SC	3.589947	3.528515	3.693555
Sum of squared residuals	3689.162	3469.350	4091.890
R-squared ¹²	0.004421	0.012166	0.004149
Adjusted R-squared	0.000527	0.008303	0.000254

Note: Because the dependent variables (Δ GLOBAL, Δ UK, Δ MADRID) are first differences of cumulative-sum series, they behave like near-white-noise innovations. In such high-frequency settings, equation-level fit statistics (R^2 , AIC, log-likelihood) will naturally appear low, since differenced random-walk-type series have little predictable structure in their short-run dynamics. In VECM analysis on such data, meaningful information instead resides in the error-correction coefficients (α) that show which variable adjusts toward equilibrium, the cointegrating vector (β) which captures the long-run relation and the impulse-response functions (IRFs) that show how shocks propagate. These diagnostics quantify equilibrium restoration and cross-series interaction, features that R^2 is not designed to measure in systems driven by near-random innovations.

¹² R-squared statistics do not carry a meaningful interpretation in VECM equations estimated in first differences. As Δy_t behaves as an innovation term, R^2 is expected to be near zero even when the error-correction dynamics are strong and statistically significant (Johansen, 1991; Juselius, 2006).

Appendix B: Vector Error Correction Estimates, Phase II

Equilibrium Relations

Term	Coefficient	Std. Error	t-Statistic
GLOBAL(-1)	1.000000	—	—
UK(-1)	1.342558	0.30047	4.46816
MADRID(-1)	0.415149	0.14851	2.79544
Constant	7.440375	—	—

Error-Correction and Short-Run Dynamics

Standard errors in parentheses; t statistics in brackets.

Term	Δ GLOBAL	Δ UK	Δ MADRID
ECT(-1)	-0.000666 (0.00048) [-1.38267]	-0.001568 (0.00048) [-3.28252]	0.001219 (0.00050) [2.45192]
Δ GLOBAL(-1)	-0.002383 (0.01179) [-0.20204]	-0.009264 (0.01169) [-0.79243]	0.007773 (0.01217) [0.63889]
Δ GLOBAL(-2)	0.005907 (0.01179) [0.50100]	0.004755 (0.01169) [0.40686]	0.004918 (0.01216) [0.40429]
Δ UK(-1)	-0.002257 (0.01189) [-0.18980]	0.009428 (0.01179) [0.79996]	-0.002612 (0.01227) [-0.21293]
Δ UK(-2)	0.009081 (0.01189) [0.76388]	0.020150 (0.01178) [1.70988]	0.016920 (0.01226) [1.37959]
Δ MADRID(-1)	-0.020952 (0.01143) [-1.83350]	-0.003631 (0.01133) [-0.32050]	0.009012 (0.01179) [0.76438]
Δ MADRID(-2)	-0.020432 (0.01143) [-1.78761]	0.003123 (0.01133) [0.27563]	-0.018109 (0.01179) [-1.53568]
Constant	-0.017166 (0.01641) [-1.04613]	0.002537 (0.01627) [0.15596]	0.016358 (0.01693) [0.96633]

Model Fit (Equation Level)

Statistic	Δ GLOBAL	Δ UK	Δ MADRID
S.E. of regression	1.391509	1.379379	1.435587
Log-likelihood	-12584.16	-12521.15	-12808.57
Akaike AIC	3.499766	3.482254	3.562136
Schwarz SC	3.507416	3.489905	3.569786
Sum of squared residuals	13918.10	13676.50	14813.82
R-squared ¹³	0.001371	0.002113	0.001609
Adj. R-squared	0.000398	0.001141	0.000637

Note: Because the dependent variables (Δ GLOBAL, Δ UK, Δ MADRID) are first differences of cumulative-sum series, they behave like near-white-noise innovations. In such high-frequency settings, equation-level fit statistics (R^2 , AIC, log-likelihood) will naturally appear low, since differenced random-walk-type series have little predictable structure in their short-run dynamics. In VECM analysis on such data, meaningful information instead resides in the error-correction coefficients (α) that show which variable adjusts toward equilibrium, the cointegrating vector (β) which captures the long-run relation and the impulse-response functions (IRFs) that show how shocks propagate. These diagnostics quantify equilibrium restoration and cross-series interaction, features that R^2 is not designed to measure in systems driven by near-random innovations.

¹³ R-squared statistics do not carry a meaningful interpretation in VECM equations estimated in first differences. As Δy_t behaves as an innovation term, R^2 is expected to be near zero even when the error-correction dynamics are strong and statistically significant (Johansen, 1991; Juselius, 2006).

Appendix C: Vector Error Correction Estimates, Phase III

Equilibrium Relations

Term	Coefficient	Std. Error	t-Statistic
GLOBAL(-1)	1.000000	—	—
UK(-1)	-0.281023	0.08232	-3.41361
MADRID(-1)	0.068891	0.04179	1.64858
Constant	-55.71245	—	—

Error-Correction and Short-Run Dynamics

Standard errors in parentheses; t statistics in brackets.

Term	Δ GLOBAL	Δ UK	Δ MADRID
ECT(-1)	-0.001440 (0.00041) [-3.53577]	0.002213 (0.00080) [2.77697]	-0.002014 (0.00064) [-3.12973]
Δ GLOBAL(-1)	-0.004361 (0.00748) [-0.58282]	0.005868 (0.01464) [0.40068]	-0.000019 (0.01182) [-0.00157]
Δ GLOBAL(-2)	-0.004959 (0.00748) [-0.66281]	0.003751 (0.01464) [0.25618]	0.004083 (0.01182) [0.34541]
Δ UK(-1)	0.010617 (0.00771) [1.37668]	0.002943 (0.01509) [0.19496]	0.007217 (0.01218) [0.59231]
Δ UK(-2)	-0.004658 (0.00771) [-0.60403]	-0.004289 (0.01509) [-0.28419]	0.009457 (0.01218) [0.77621]
Δ MADRID(-1)	-0.004339 (0.00750) [-0.57881]	-0.017934 (0.01467) [-1.22250]	-0.004165 (0.01184) [-0.35170]
Δ MADRID(-2)	0.000791 (0.00750) [0.10556]	-0.005519 (0.01467) [-0.37617]	-0.005907 (0.01184) [-0.49879]
Constant	0.000249 (0.01075) [0.02314]	0.000380 (0.02105) [0.01806]	0.000413 (0.01699) [0.02429]

Model Fit (Equation Level)

Statistic	Δ GLOBAL	Δ UK	Δ MADRID
S.E. of regression	1.442374	2.822910	2.278837
Log-likelihood	-32126.54	-44211.81	-40358.38
Akaike AIC	3.570902	4.913858	4.485652
Schwarz SC	3.574368	4.917324	4.489118
Sum of squared residuals	37,427.14	143,359.10	93,423.81
R-squared ¹⁴	0.000899	.000899	.000899
Adj. R-squared	0.000511	0.000511	0.000511

Note: Because the dependent variables (Δ GLOBAL, Δ UK, Δ MADRID) are first differences of cumulative-sum series, they behave like near-white-noise innovations. In such high-frequency settings, equation-level fit statistics (R^2 , AIC, log-likelihood) will naturally appear low, since differenced random-walk-type series have little predictable structure in their short-run dynamics. In VECM analysis on such data, meaningful information instead resides in the error-correction coefficients (α) that show which variable adjusts toward equilibrium, the cointegrating vector (β) which captures the long-run relation and the impulse-response functions (IRFs) that show how shocks propagate. These diagnostics quantify equilibrium restoration and cross-series interaction, features that R^2 is not designed to measure in systems driven by near-random innovations.

¹⁴ R-squared statistics do not carry a meaningful interpretation in VECM equations estimated in first differences. As Δy_t behaves as an innovation term, R^2 is expected to be near zero even when the error-correction dynamics are strong and statistically significant (Johansen, 1991; Juselius, 2006).

Appendix D: Vector Error Correction Estimates, Phase IV

Equilibrium Relations

Term	Coefficient	Std. Error	t-Statistic
GLOBAL(-1)	1.000000	—	—
UK(-1)	-6.202646	(2.22077)	-2.79302
MADRID(-1)	-2.186844	(0.87642)	-2.49521
Constant	-837.1920	—	—

Error-Correction and Short-Run Dynamics

Standard errors in parentheses; t statistics in brackets.

Term	Δ GLOBAL	Δ UK	Δ MADRID
ECT(-1)	-0.000075 (0.000056) [-1.33930]	0.000148 (0.000056) [2.65342]	0.000134 (0.000055) [2.43632]
Δ GLOBAL(-1)	-0.017741 (0.00962) [-1.84358]	0.000653 (0.00961) [0.06797]	0.007609 (0.00942) [0.80806]
Δ GLOBAL(-2)	0.009781 (0.00962) [1.01635]	0.005965 (0.00961) [0.62062]	-0.016491 (0.00942) [-1.75114]
Δ UK(-1)	0.000165 (0.00964) [0.01716]	0.001069 (0.00962) [0.11109]	-0.002346 (0.00943) [-0.24880]
Δ UK(-2)	-0.012032 (0.00964) [-1.24874]	-0.001470 (0.00962) [-0.15274]	0.014875 (0.00943) [1.57766]
Δ MADRID(-1)	-0.001108 (0.00983) [-0.11271]	0.000736 (0.00982) [0.07495]	0.002380 (0.00962) [0.24730]
Δ MADRID(-2)	0.029425 (0.00983) [2.99242]	-0.017357 (0.00982) [-1.76733]	0.004892 (0.00962) [0.50842]
Constant	-0.006565 (0.01354) [-0.48481]	-0.003973 (0.01352) [-0.29375]	-0.021198 (0.01325) [-1.59978]

Model Fit (Equation Level)

Statistic	Δ GLOBAL	Δ UK	Δ MADRID
S.E. of regression	1.406588	1.404876	1.376450
Log-likelihood	-18,999.86	-18,986.71	-18,766.00
Akaike AIC	3.520952	3.518516	3.477633
Schwarz SC	3.526351	3.523916	3.483032
Sum of squared residuals	21,345.93	21,294.01	20,440.99
R-squared ¹⁵	0.001549	0.000968	0.001157
Adj. R-squared	0.000902	0.000319	0.000509

Note: Because the dependent variables (Δ GLOBAL, Δ UK, Δ MADRID) are first differences of cumulative-sum series, they behave like near-white-noise innovations. In such high-frequency settings, equation-level fit statistics (R^2 , AIC, log-likelihood) will naturally appear low, since differenced random-walk-type series have little predictable structure in their short-run dynamics. In VECM analysis on such data, meaningful information instead resides in the error-correction coefficients (α) that show which variable adjusts toward equilibrium, the cointegrating vector (β) which captures the long-run relation and the impulse-response functions (IRFs) that show how shocks propagate. These diagnostics quantify equilibrium restoration and cross-series interaction, features that R^2 is not designed to measure in systems driven by near-random innovations.

¹⁵ R-squared statistics do not carry a meaningful interpretation in VECM equations estimated in first differences. As Δy_t behaves as an innovation term, R^2 is expected to be near zero even when the error-correction dynamics are strong and statistically significant (Johansen, 1991; Juselius, 2006).

Appendix E: Johansen Cointegration Results

Table E1: Johansen Trace Test, Phase I

Hypothesised No. of CE(s)	Eigenvalue	Trace Statistic	0.05 Critical Value	p-value	Decision
None*	0.012599	38.88156	35.01090	0.0183	Reject ($r = 0$)
At most 1	0.005733	16.11084	18.39771	0.1015	Do not reject
At most 2*	0.003216	5.784844	3.841465	0.0162	Reject (artifact of small eigenvalue)

Conclusion (Trace test): Rank = 1 at 5% level.

* MacKinnon-Haug-Michelis (1999) p-values reported.

Table E2: Johansen Trace Test, Phase III

Hypothesised No. of CE(s)	Eigenvalue	Trace Statistic	0.10 Critical Value	p-value	Decision
None*	0.002459	29.49124	27.06695	0.0542	Reject at 10%
At most 1	0.001407	11.77895	13.42878	0.1678	Do not reject
At most 2	0.000229	1.647479	2.705545	0.1993	Do not reject

Conclusion (Trace test): Rank = 1 at 10% level.

* MacKinnon-Haug-Michelis (1999) p-values reported.